

# Supplementary Information for “The Effect of Structural and Chemical Bonding Change on Optical Properties of Si/Si<sub>1-x</sub>C<sub>x</sub> Core/Shell Nanowires”

Woo-Jung Lee<sup>1</sup>, Jin Won Ma<sup>1</sup>, Jung Min Bae<sup>1</sup>, Kwang-Sik Jeong<sup>1</sup>, Mann-Ho Cho<sup>1,\*</sup>, Chul Lee<sup>2</sup>, Eun Jip Choi<sup>2</sup>, Chul Kang<sup>3</sup>

<sup>1</sup>*Department of Physics and Applied Physics, Yonsei University, Seoul 120-749, Korea*

<sup>2</sup>*Department of physics, University of Seoul, Seoul 130-743, Korea, Korea*

<sup>3</sup>*Advanced Photonics Research Institute, Gwangju Institute of Science and Technology, Gwangju, 500-712*

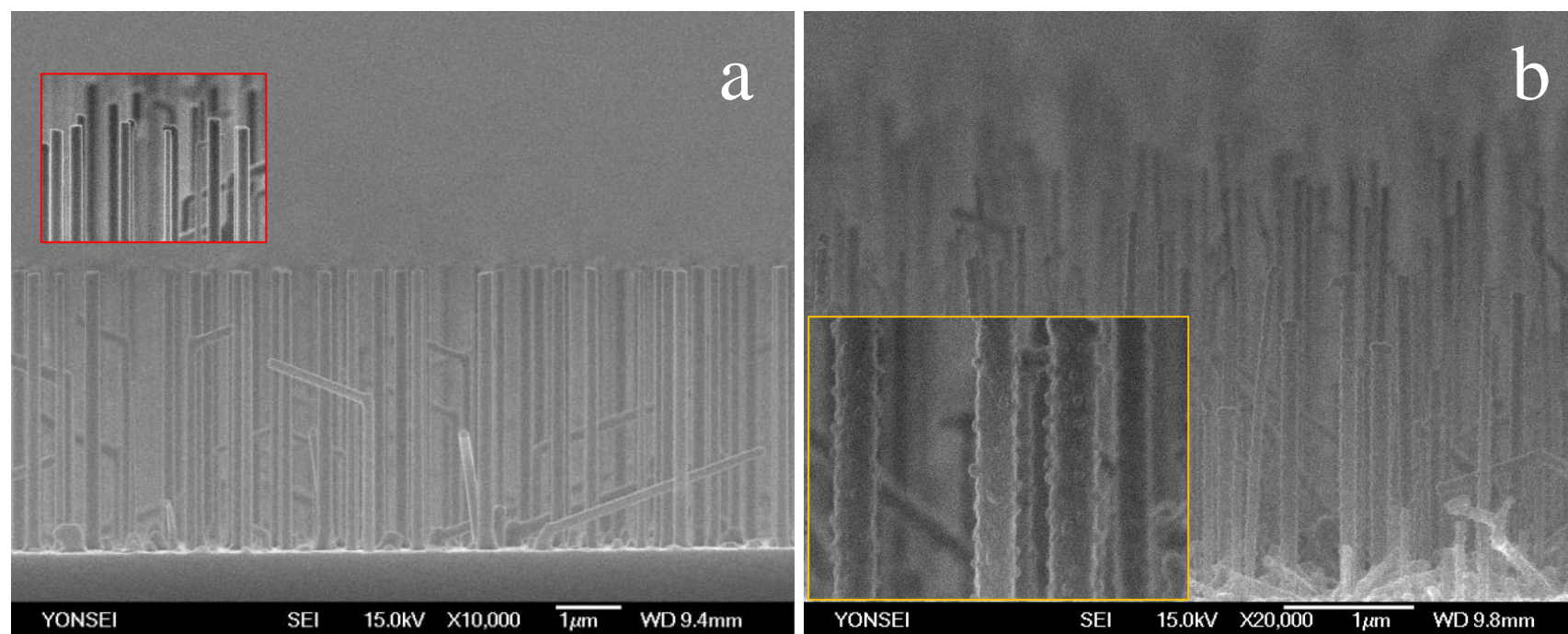


Figure S1. FE-SEM images of the Si/Si<sub>1-x</sub>C<sub>x</sub> core/shell. (a) as-grown Si core NW after the removal of the Au tip at top of the wire, and (b) Si/Si<sub>1-x</sub>C<sub>x</sub> core/shell NWs annealed at 750 °C in a vacuum.

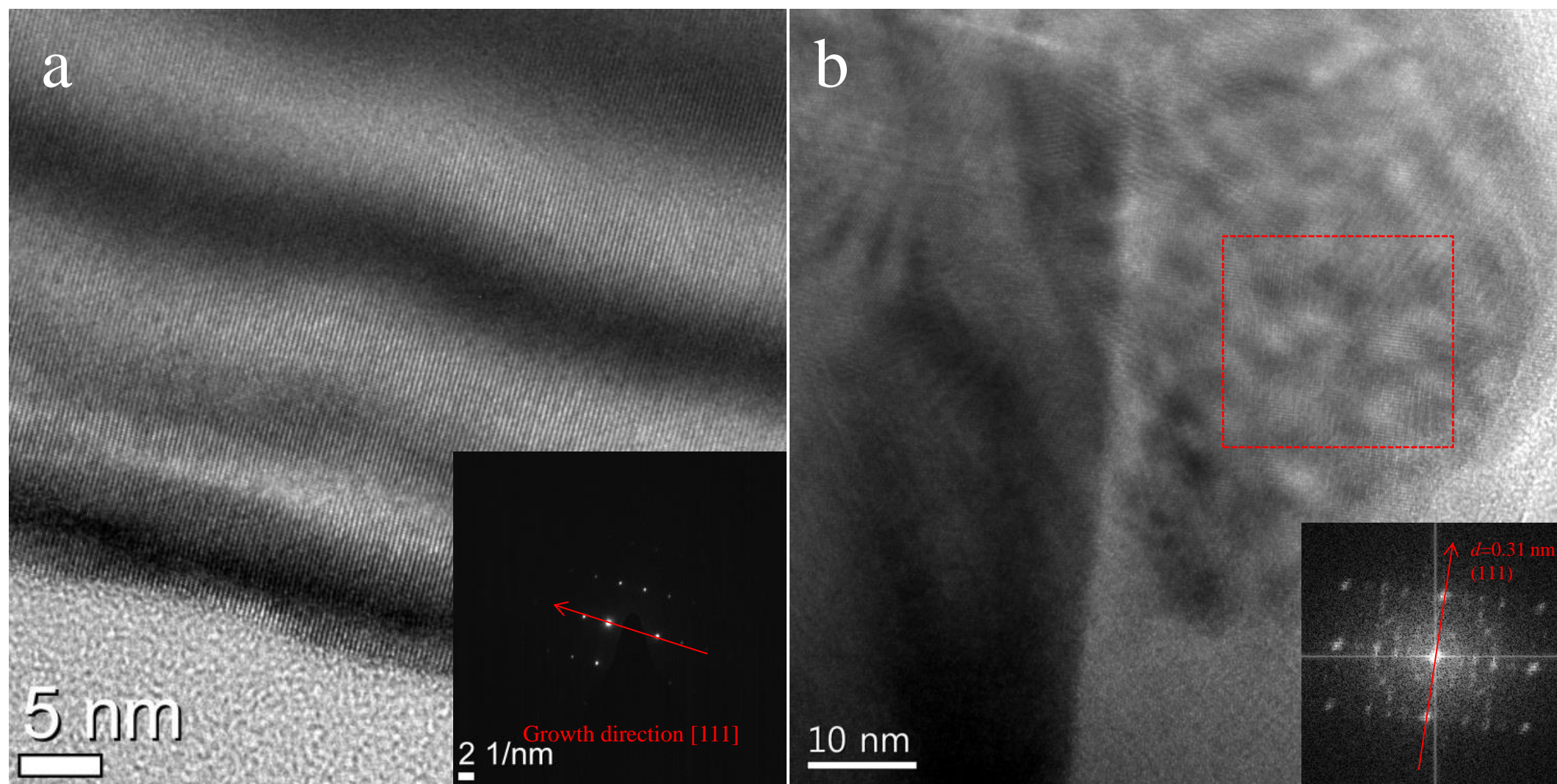


Figure S2. (a) HR-TEM image of as-grown Si core NW after the removal of the Au tip at top of the wire, which presents single crystal structure. (b) HR-TEM image of Si/Si<sub>1-x</sub>C<sub>x</sub> core/shell NWs annealed at 600 °C in a vacuum. In this case, Si<sub>1-x</sub>C<sub>x</sub> shell became thick and poly-crystallization.

Supporting Figure S2. Lee *at. al.*

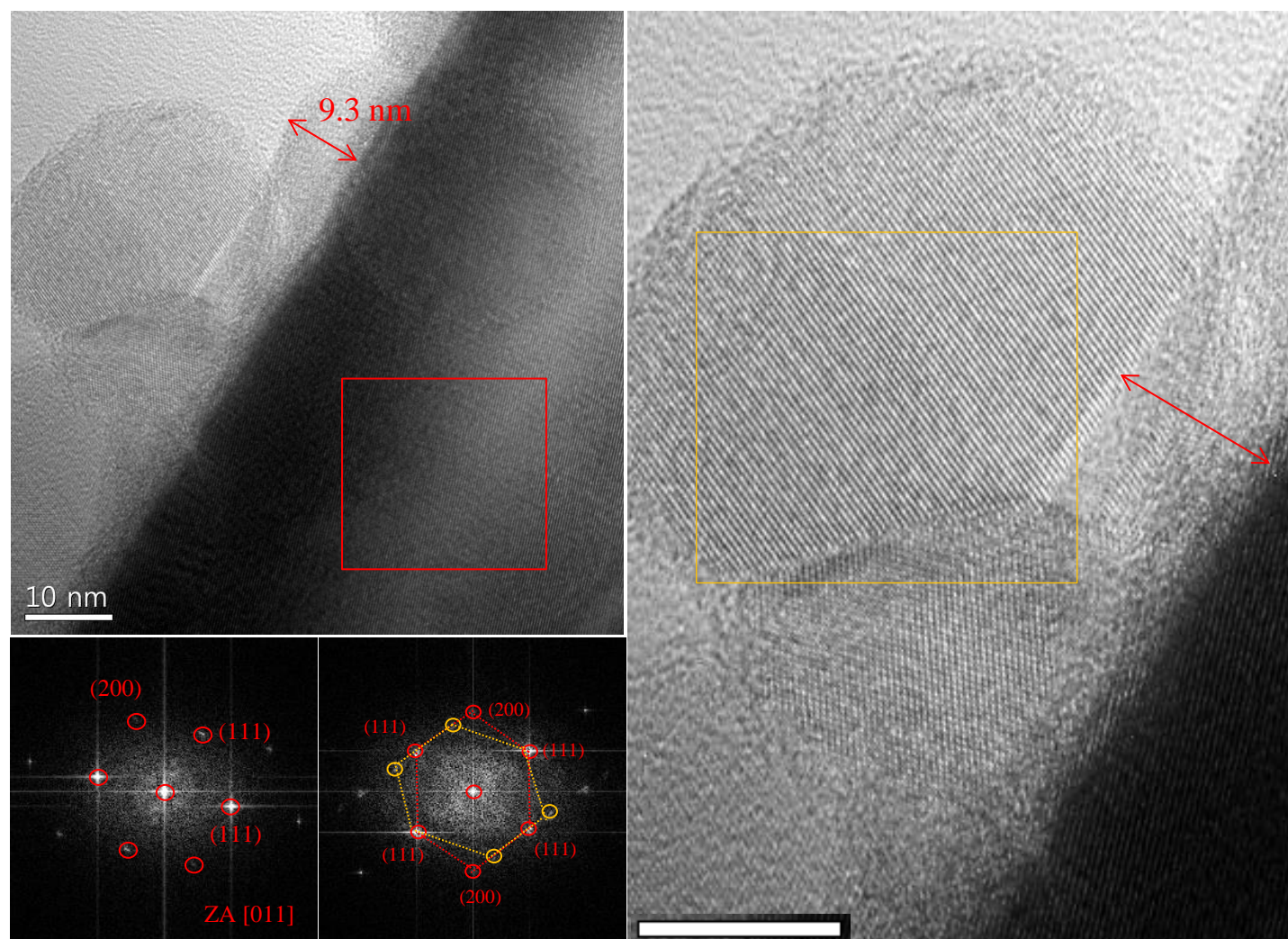


Figure S3. HR-TEM images of the Si/Si<sub>1-x</sub>C<sub>x</sub> core/shell NWs annealed at 750 °C in a vacuum. In this case, Si<sub>1-x</sub>C<sub>x</sub> shell was transformed into single crystal structure.

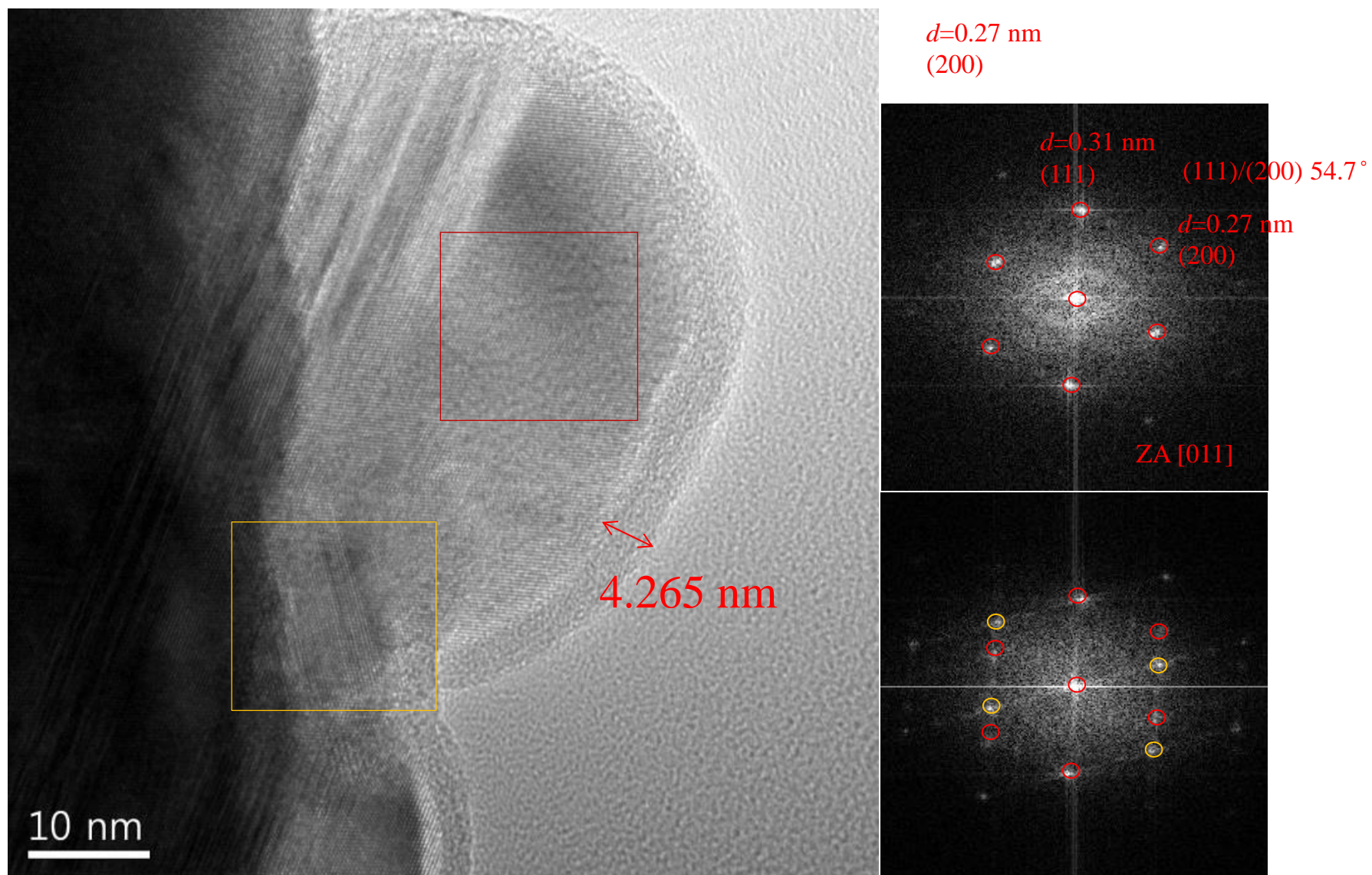


Figure S4. HR-TEM images of the Si/Si<sub>1-x</sub>C<sub>x</sub> core/shell NWs annealed at 750 °C in a vacuum. In this case, Si<sub>1-x</sub>C<sub>x</sub> shell was transformed into single crystal structure with an amount of twin defect.

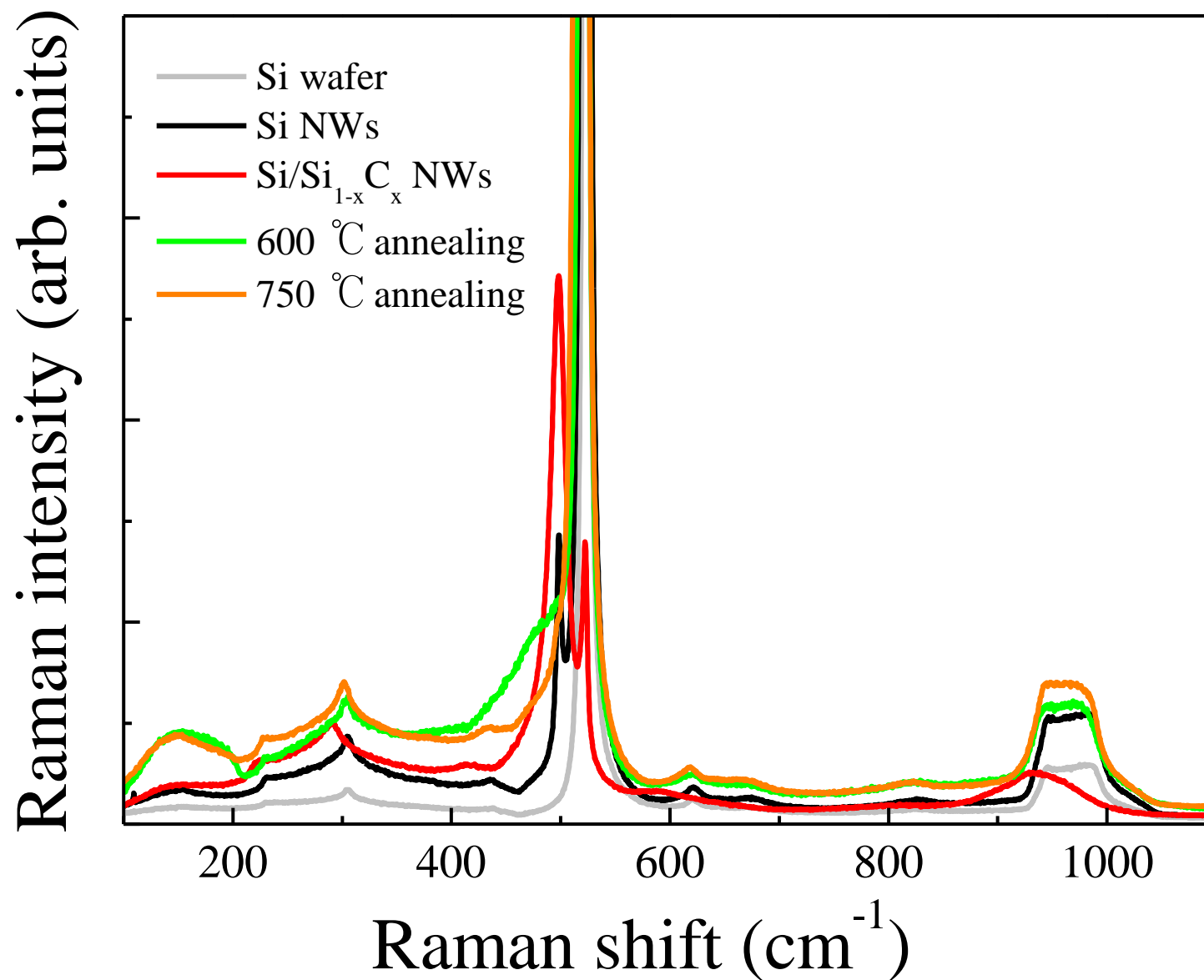
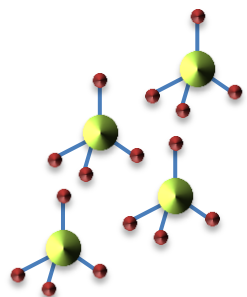
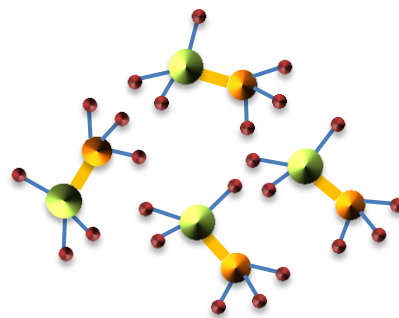
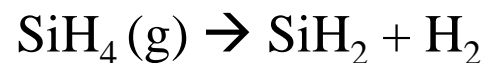


Figure S5. Raman spectra of the Si/Si<sub>1-x</sub>C<sub>x</sub> core/shell NWs as a function of annealing temperature in wide range from 100 ~ 1100 cm<sup>-1</sup>.



*SiH<sub>4</sub> gases decomposition*



*SiH<sub>3</sub>CH<sub>3</sub> gases decomposition*



### **Si<sub>1-x</sub>C<sub>x</sub> Film Growth**

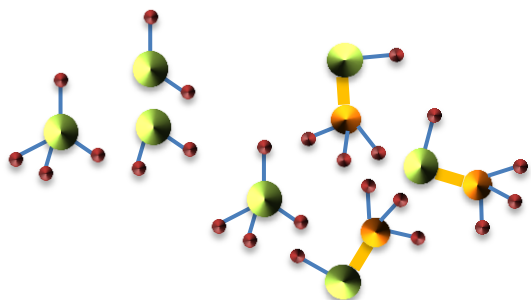


Figure S6. A schematic diagram of possible decomposition pathways in the gas phase reactions of SiH<sub>4</sub> with CH<sub>3</sub>SiH<sub>3</sub> for Si<sub>1-x</sub>C<sub>x</sub> shell growth on Si core NW.

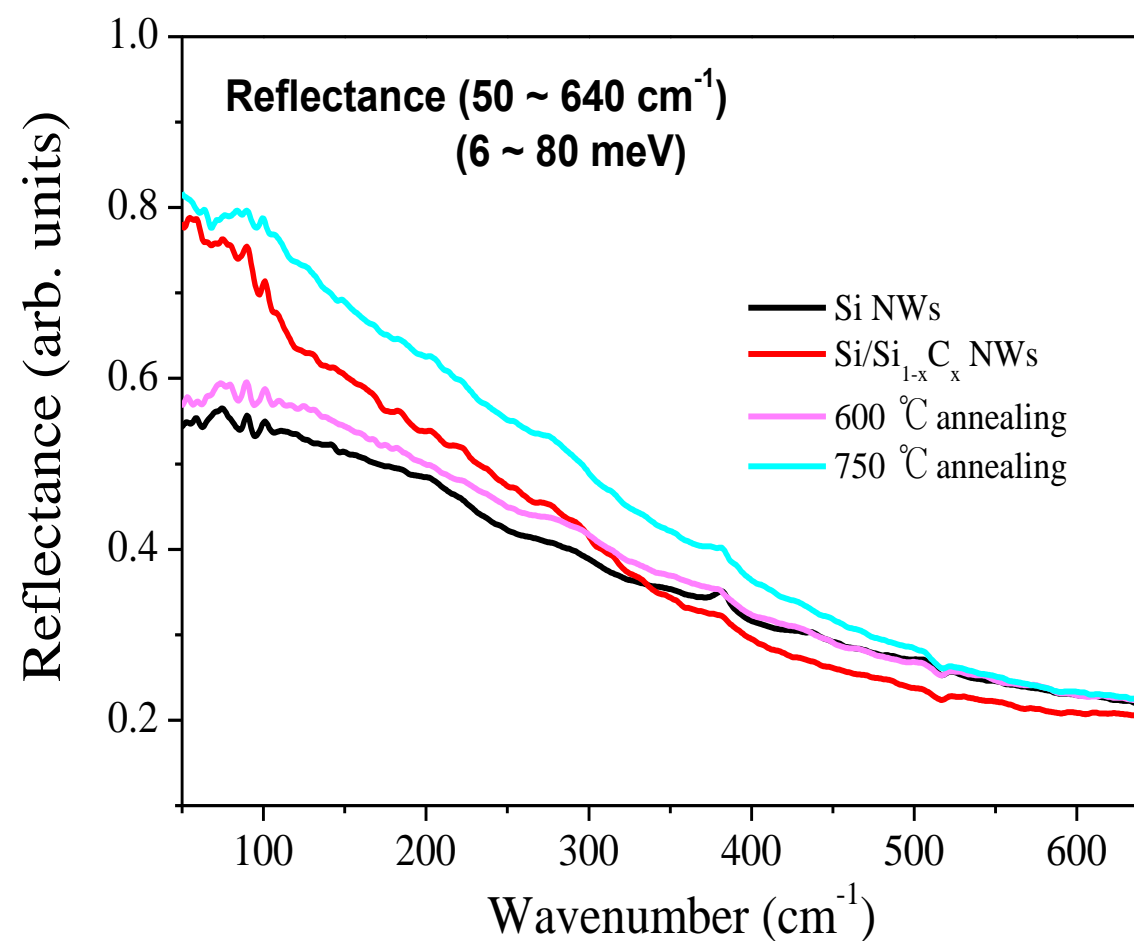


Figure S7. The reflectance spectra in far-infrared region of the Si/Si<sub>1-x</sub>C<sub>x</sub> core/shell NWs as a function of annealing temperature.



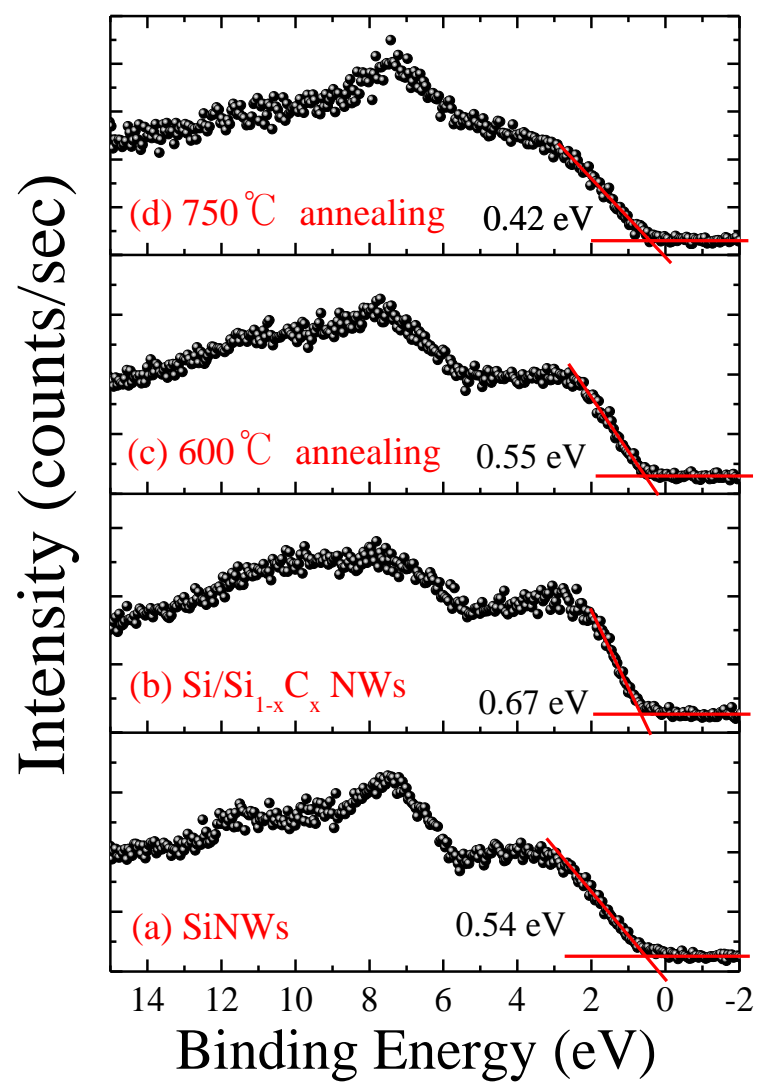


Figure S8. The valence band measured from the Si/Si<sub>1-x</sub>C<sub>x</sub> core/shell NWs as a function of annealing temperature by using XPS.

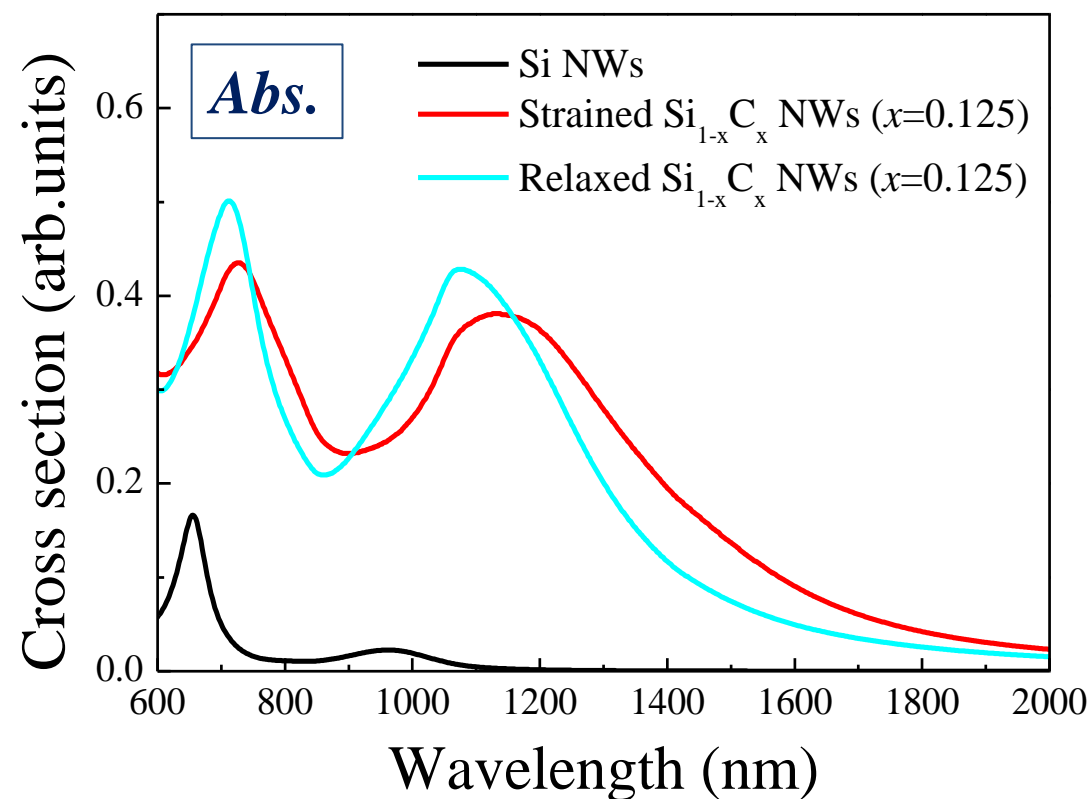


Figure S9. After the irradiation of light source (790 nm), absorption of the Si and Si<sub>1-x</sub>C<sub>x</sub> NW was attained by the result of 2-D FDTD. The Si<sub>1-x</sub>C<sub>x</sub> NW was classified into two kinds; one is strained Si<sub>1-x</sub>C<sub>x</sub> NW including substitutional C atoms randomly distributed in Si lattices and the other is relaxed Si<sub>1-x</sub>C<sub>x</sub> NW consisting of 3nn configuration of C atoms locally existed in Si lattices.